CORRECTED 2 MAY 2024; SEE FULL TEXT

NEURODEVELOPMENT

Balancing act of small GTPases downstream of plexin-A4 signaling motifs promotes dendrite elaboration in mammalian cortical neurons

Oday Abushalbaq[1], Jiyeon Baek[1], Avraham Yaron[2], Tracy S. Tran[1]*

The precise development of neuronal morphologies is crucial to the establishment of synaptic circuits and, ultimately, proper brain function. Signaling by the axon guidance cue semaphorin 3A (Sema3A) and its receptor complex of neuropilin-1 and plexin-A4 has multifunctional outcomes in neuronal morphogenesis. Downstream activation of the RhoGEF FARP2 through interaction with the lysine-arginine-lysine motif of plexin-A4 and consequent activation of the small GTPase Rac1 promotes dendrite arborization, but this pathway is dispensable for axon repulsion. Here, we investigated the interplay of small GTPase signaling mechanisms underlying Sema3A-mediated dendritic elaboration in mouse layer V cortical neurons in vitro and in vivo. Sema3A promoted the binding of the small GTPase Rnd1 to the amino acid motif leucine-valine-serine (LVS) in the cytoplasmic domain of plexin-A4. Rnd1 inhibited the activity of the small GTPase RhoA and the kinase ROCK, thus supporting the activity of the GTPase Rac1, which permitted the growth and branching of dendrites. Overexpression of a dominant-negative RhoA, a constitutively active Rac1, or the pharmacological inhibition of ROCK activity rescued defects in dendritic elaboration in neurons expressing a plexin-A4 mutant lacking the LVS motif. Our findings provide insights into the previously unappreciated balancing act between Rho and Rac signaling downstream of specific motifs in plexin-A4 to mediate Sema3A-dependent dendritic elaboration in mammalian cortical neuron development.

INTRODUCTION

The formation of distinct neuronal morphologies is tightly connected to their functions (*1*). In particular, it is crucial for developing neurons to establish proper dendritic branching patterns and densities to ensure that the correct number of functional synapses is formed. The formation of abnormal neuronal connections, impaired dendrite morphology in particular, has been shown to contribute to neurodevelopmental and neurological disorders, including intellectual disability (*2*, *3*), autism spectrum disorder (*4*), schizophrenia (*5*), and epilepsy (*6*).

The neurodevelopmental processes of neurite outgrowth, for both dendrites and axons, are largely dependent on and initiated by a number of factors that include cell-cell adhesion, extracellular matrix adhesion, and extracellular guidance cues. These factors mediate functions by regulating cytoskeletal components, actin and microtubules, leading to morphological changes in neurites (*7*, *8*). The class 3 secreted semaphorins (Sema3s) are among the most studied guidance cues in the developing mammalian nervous system because of their compelling multifunctionality and link to downstream cytoskeletal components. In particular, Sema3A has been demonstrated to bind and activate the same holoreceptor complex of neuropilin-1 (Nrp1) and plexin-A4 to promote axonal repulsion and dendritic morphogenesis in different neuronal populations both in vitro and in vivo (*9*–*13*). It was shown that *PlxnA4*$^{-/-}$ or *PlxnA3*$^{-/-}$/*PlxnA4*$^{-/-}$ double-mutant mice exhibit exuberant axonal projections in dorsal root ganglion sensory neurons (*13*), and both *Nrp1*$^{Sema-}$ (a mutated receptor that cannot bind to Sema3A) and *PlxnA4*$^{-/-}$ animals displayed severe reductions in basal dendrite outgrowth of layer V cortical pyramidal neurons (*10*, *12*). However, the underlying signaling mechanisms that enable the same ligand/receptor complex (Sema3A-Nrp1/plexin-A4) to mediate such disparate functions are largely unknown. The complexity of the cytoplasmic domain in plexin-A4 may mediate the disparate cellular responses observed upon the receptor's activation by Sema3A. Previously, we performed an in vitro structure-function analysis and identified several cytoplasmic domains or motifs involved in dendritic elaboration and axon guidance (*11*). We identified three amino acids, Lys-Arg-Lys (hereafter, KRK), in the cytoplasmic domain that are required for the binding of band 4.1, ezrin, radixin, and moesin (FERM) domain–containing Rho guanine nucleotide exchange factor (GEF) proteins, including FERM, ARHGEF, and pleckstrin domain-containing protein 1 (FARP1) and FARP2 (*14*, *15*), and are sufficient to enable Sema3A-induced cortical neuron dendritic elaboration in vitro (*11*). In addition, the KRK motif is necessary for Sema3A-induced, Nrp1/plexin-A4–mediated dendritic morphogenesis, but not axonal repulsion, in cortical layer V pyramidal neurons and does so by associating with the GEF FARP2 leading to the activation of the small guanosine triphosphatase (GTPase) Rac1 (*16*). Although several other Rho GTPases—including but not limited to RhoA, RhoD, and Rnd1—are known to either associate with or be downstream of plexin-A signaling to mediate different cellular processes (*17*–*20*), it is not known whether any of these small GTPases are also required for dendritic morphogenesis in response to Sema3A.

Several of these Rho GTPases bind to the Hinge/Rho binding domain (H/RBD) region of plexin-A receptors, which has been revealed to be crucial for releasing the autoinhibition of the C1 and C2 GTPase activating protein (GAP)–like domains of the receptor and allowing activation of the receptor (*21*–*24*). Of the several Rho GTPases that bind the H/RBD domain of plexin-A family members, Rnd1 is of particular interest because of its low intrinsic GTPase activity, which renders it constitutively active and functionally regulated mainly by its expression and cellular localization (*25*, *26*). Rnd1 promotes the rearrangement of the actin and microtubule

[1]Department of Biological Sciences, Rutgers University, Newark, NJ 07102, USA. [2]Department of Biomolecular Sciences and Department of Molecular Neuroscience, Weizmann Institute of Science, Rehovot 76100, Israel.
*Corresponding author. Email: tstran@rutgers.edu

dynamics (*26*), leading to dendrite elaboration (*27*) and dendritic spine elongation (*28*) in rat hippocampal neurons through inactivation of the RhoA–Rho-associated protein kinase (ROCK) pathway (*26*, *28*–*36*). Previously, Rnd1 has been characterized to associate with the H/RBD region of plexin-A1, which contains the conserved amino acid motif leucine-valine-serine (LVS) (*23*, *37*, *38*), and plexin-B1 (*19*, *37*, *39*); its association with plexin-A1 induces axonal repulsion (*15*). However, it is not known whether Rnd1 also interacts with plexin-A4 at the LVS motif and whether this interaction contributes to neuronal dendrite elaboration.

Here, we generated a new, genetically modified mouse line, $PlxnA4^{LVS\text{-}GGA}$, wherein the LVS amino acid motif was substituted with GGA in the H/RBD region of plexin-A4 using the CRISPR-Cas9 gene editing method. Using this mouse line, we investigated whether the LVS motif is required for Sema3A/plexin-A4–induced cortical pyramidal neuron dendritic development in vivo and in vitro. The results suggest independent and cross-talking Rho GTPase–mediated pathways that coordinate Sema3A-dependent dendritic branching and growth in cortical neuron development.

RESULTS

Generation and validation of $PlxnA4^{LVS\text{-}GGA/LVS\text{-}GGA}$ mutant mouse line

To investigate the requirement of the LVS motif of plexin-A4 in Sema3A-Nrp1/plexin-A4–induced dendritic elaboration, we generated a novel mouse mutant, using CRISPR-Cas9 technology, to specifically target the sequence encoding the LVS motif in the plexin-A4 locus with the substitution of GGA ($PlxnA4^{LVS\text{-}GGA/LVS\text{-}GGA}$). The LVS nucleotide sequence (5′-TTAGTGTCC-3′) was substituted with GGA (5′-GGAGGGGCC-3′). The specificity of the desired mutation was confirmed using DNA sequencing (Fig. 1A) and tail tip genomic DNA polymerase chain reaction (PCR) genotyping (Fig. 1B). Total plexin-A4 protein levels were also evaluated using biochemical analysis in the mutant mouse line. Plexin-A4 protein levels in $PlxnA4^{LVS\text{-}GGA/LVS\text{-}GGA}$ adult animal cortices were comparable to wild-type (WT) littermates ($PlxnA4^{+/+}$) and heterozygotes ($PlxnA4^{+/LVS\text{-}GGA}$; Fig. 1C). Moreover, the $PlxnA4^{LVS\text{-}GGA/LVS\text{-}GGA}$ mutation did not affect the dendritic localization of plexin-A4 receptor compared with WT neurons immunostained for plexin-A4 under conditions without Triton X-100 (Fig. 1D). Last, the association between plexin-A4 and its coreceptor Nrp1 remained intact and at comparable levels between $PlxnA4^{+/+}$ *and* $PlxnA4^{LVS\text{-}GGA/LVS\text{-}GGA}$ brains (Fig. 1E). These findings suggest that the LVS-to-GGA mutation did not affect the expression and distribution of plexin-A4 in cortical neurons or the holoreceptor formation between Nrp1 and plexin-A4, enabling us to use the mutant mouse line in this study.

The LVS motif in the H/RBD domain of plexin-A4 receptor is required for dendritic elaboration in cortical pyramidal neurons in vivo

To investigate whether the LVS motif in the H/RBD domain of plexin-A4 receptor is necessary for cortical pyramidal neuron dendritic morphogenesis, we used adult brain tissue from $PlxnA4^{LVS\text{-}GGA/LVS\text{-}GGA}$ mutant mice (2 to 3 months old) to assess the dendritic morphology of deep layer cortical pyramidal neurons using the unbiased Golgi staining in comparison to $PlxnA4^{-/-}$ and WT $PlxnA4^{+/+}$ brains. Dendritic morphology assessment was done using well-established methods (*16*) such as number of dendritic intersections (Sholl analysis), dendritic length, and dendritic complexity. Our findings show impaired dendritic morphology of basal dendrites of deep-layer cortical pyramidal neurons in $PlxnA4^{LVS\text{-}GGA/LVS\text{-}GGA}$ animals, as also observed in $PlxnA4^{-/-}$ animals, in comparison with $PlxnA4^{+/+}$ animals that exhibit a normal dendritic phenotype in vivo (Fig. 2A). Sholl analysis showed significant impairments in dendritic morphology in both $PlxnA4^{LVS\text{-}GGA/LVS\text{-}GGA}$ and $PlxnA4^{-/-}$ animals (Fig. 2B). Consistent differences in $PlxnA4^{LVS\text{-}GGA/LVS\text{-}GGA}$ and $PlxnA4^{-/-}$ in comparison with $PlxnA4^{+/+}$ were also found in total dendritic length (Fig. 2C) and dendritic complexity (Fig. 2D). These results demonstrate that the LVS motif of plexin-A4 is essential for dendritic elaboration in cortical neurons in vivo.

The LVS motif in the H/RBD domain of plexin-A4 is required for Sema3A/plexin-A4–induced dendritic elaboration in cortical pyramidal neurons in vitro

Next, to test whether the LVS motif in plexin-A4 increases dendritic elaboration specifically through Sema3A signaling, we addressed the role of the LVS motif in Sema3A-induced plexin-A4 activation in cortical pyramidal neurons in vitro. Primary cortical neurons were cultured from $PlxnA4^{LVS\text{-}GGA/LVS\text{-}GGA}$ and $PlxnA4^{+/+}$ (control) mice on embryonic day 13.5 (E13.5) in neurobasal medium for 5 days. Cortical neurons from the two genotypes were then stimulated with either alkaline phosphatase (AP) alone or AP-Sema3A (5 nM) for 24 hours to induce dendritic elaboration; then immunostained with antibody to microtubule associated protein 2 (MAP2), a dendritic marker (*11*, *16*); and assessed for the number of dendritic intersections, total dendritic length, and dendritic complexity.

$PlxnA4^{LVS\text{-}GGA/LVS\text{-}GGA}$ cortical neurons were unresponsive to Sema3A-induced dendritic elaboration, as has been previously shown in $PlxnA4^{-/-}$ neurons overexpressing $PlxnA4^{LVS\text{-}GGA/LVS\text{-}GGA}$ (*11*, *16*), in comparison with $PlxnA4^{+/+}$ neurons that exhibit an increase in the number of dendritic branches in response to Sema3A treatment (fig. S1A). Sholl analysis showed a significant decrease in dendritic intersections in $PlxnA4^{LVS\text{-}GGA/LVS\text{-}GGA}$ neurons compared with $PlxnA4^{+/+}$ neurons in response to Sema3A treatment (fig. S1B). Consistent with the Sholl analysis results, the $PlxnA4^{LVS\text{-}GGA/LVS\text{-}GGA}$ neurons exhibited decreased total dendritic length and dendritic complexity index (DCI; fig. S1B) compared with the control neurons in response to Sema3A treatment. The current findings are in line with our previous in vitro structure-function screen (*11*) and our in vivo findings (Fig. 2, A to D). Collectively, our findings demonstrate that the LVS motif in the H/RBD region of plexin-A4 facilitates Sema3A-induced dendritic morphogenesis in cortical pyramidal neurons during development.

The Rho GTPase Rnd1 associates with the LVS motif of plexin-A4 and is necessary for Sema3A/plexin-A4–mediated dendritic elaboration

Next, we aimed to address the signaling downstream of the LVS motif that mediates Sema3A-induced dendritic elaboration. The Rho GTPase Rnd1 is known to interact with the H/RBD region of other plexins, namely, plexin-A1 (*37*, *38*) and plexin-B1 (*19*, *37*, *39*). Whether Rnd1 also interacts with plexin-A4 and whether the LVS motif is required for this interaction to induce dendrite elaboration are not known.

To examine the role of Rho GTPase Rnd1 in Sema3A-induced dendritic elaboration, we first examined whether Rnd1 can associate with WT plexin-A4 and whether the LVS motif is required for

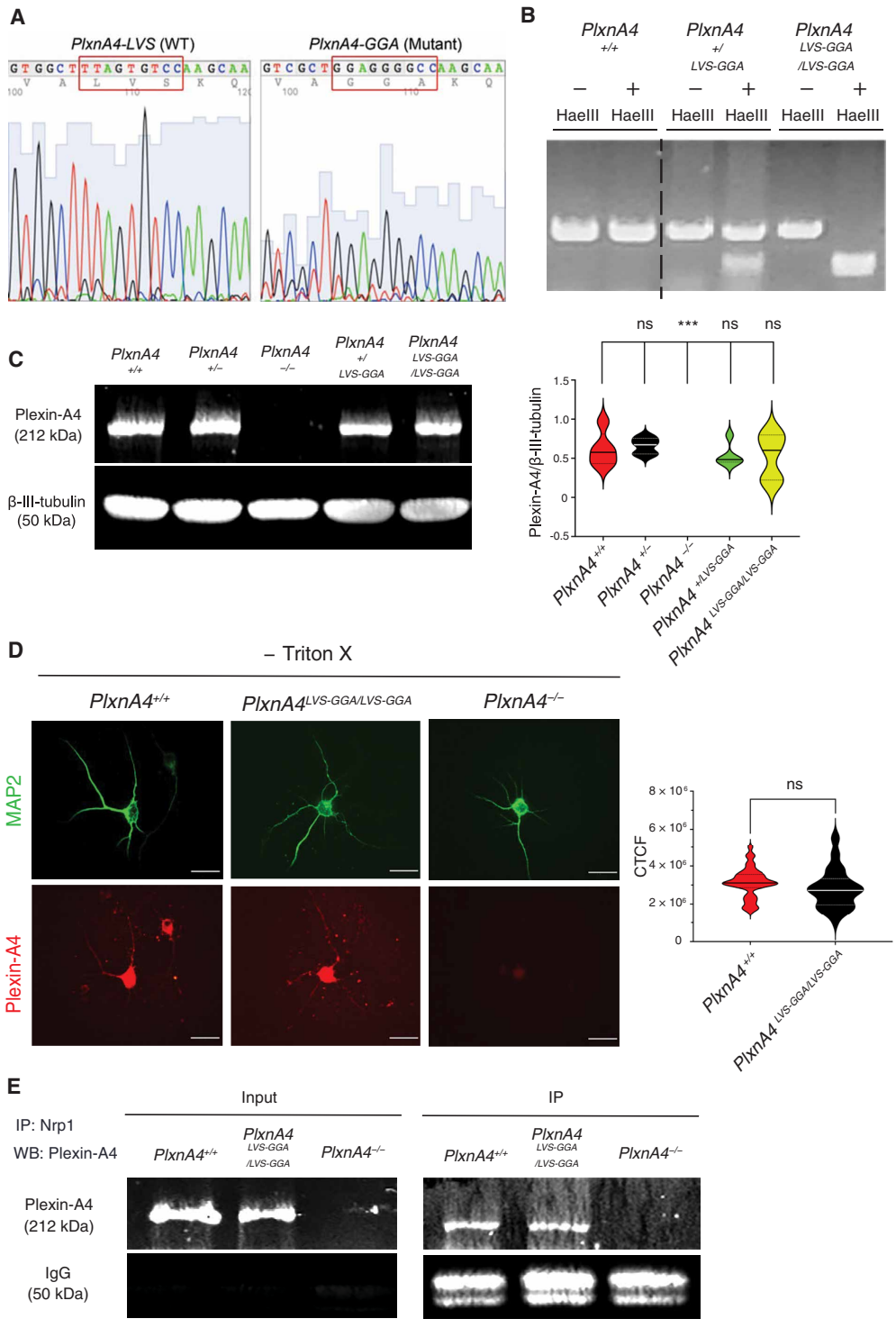

Fig. 1. Validation of the *PlxnA4*$^{LVS\text{-}GGA/LVS\text{-}GGA}$ mutant mouse line. (**A**) Genomic DNA sequencing shows the specific substitution of the LVS amino acid sequence to GGA in the endogenous plexin-A4 receptor. WT, wild type. (**B**) PCR analysis of tail genomic DNA from *PlxnA4*$^{LVS\text{-}GGA/LVS\text{-}GGA}$, *PlxnA4*$^{+/LVS\text{-}GGA}$, and *PlxnA4*$^{-/-}$ mice aged P21 to P27. Dashed line indicates where two images, each from separate gels, have been combined. (**C**) Western blot analysis of adult cortices extracted from *PlxnA4*$^{LVS\text{-}GGA/LVS\text{-}GGA}$, *PlxnA4*$^{+/LVS\text{-}GGA}$, *PlxnA4*$^{+/-}$, *PlxnA4*$^{-/-}$, and *PlxnA4*$^{+/+}$ mice, with quantification of plexin-A4 protein levels relative to input control β-tubulin. Data are means ± SEM from $n = 5$ animals per genotype. $^{ns}P > 0.05$ (not significant) and $^{***}P < 0.001$ by one-way ANOVA and Tukey's post hoc analysis. (**D**) Primary cortical neurons from *PlxnA4*$^{LVS\text{-}GGA/LVS\text{-}GGA}$, wild-type (*PlxnA4*$^{+/+}$), and *PlxnA4*$^{-/-}$ embryos were immunostained with antibodies to plexin-A4 and MAP2 in the absence of Triton X-100, and plexin-A4 immunofluorescence levels were quantified. CTCF, corrected total cell fluorescence. Data are means ± SEM from 20 neurons from each of $n = 2$ animals per genotype. Scale bars, 20 μm. $^{ns}P > 0.05$ (not significant) by Student's t test. (**E**) Immunoblotting for the indicated proteins after immunoprecipitation for Nrp1 in cortical lysates from *PlxnA4*$^{LVS\text{-}GGA/LVS\text{-}GGA}$, *PlxnA4*$^{-/-}$, and *PlxnA4*$^{+/+}$ mice. Blots are representative of $n = 2$ animals per genotype.

this association. First, cortical neurons from *PlxnA4*$^{LVS\text{-}GGA/LVS\text{-}GGA}$, *PlxnA4*$^{-/-}$, and *PlxnA4*$^{+/+}$ E13.5 embryos were isolated and cultured for 5 days and were treated with either AP alone or AP-Sema3A for 15 min, followed by protein lysate collection. The total protein lysates from each sample were then subjected to immunoprecipitation (IP) with antibody to plexin-A4 and were probed with antibody to Rnd1 in Western blot analysis. Our results showed that AP-Sema3A treatment was able to induce increased Rnd1 association with the WT plexin-A4 receptor compared with AP-alone control treatment from the *PlxnA4*$^{+/+}$ control neurons. On the other hand, AP-Sema3A treatment was unable to promote more association between Rnd1 and plexin-A4

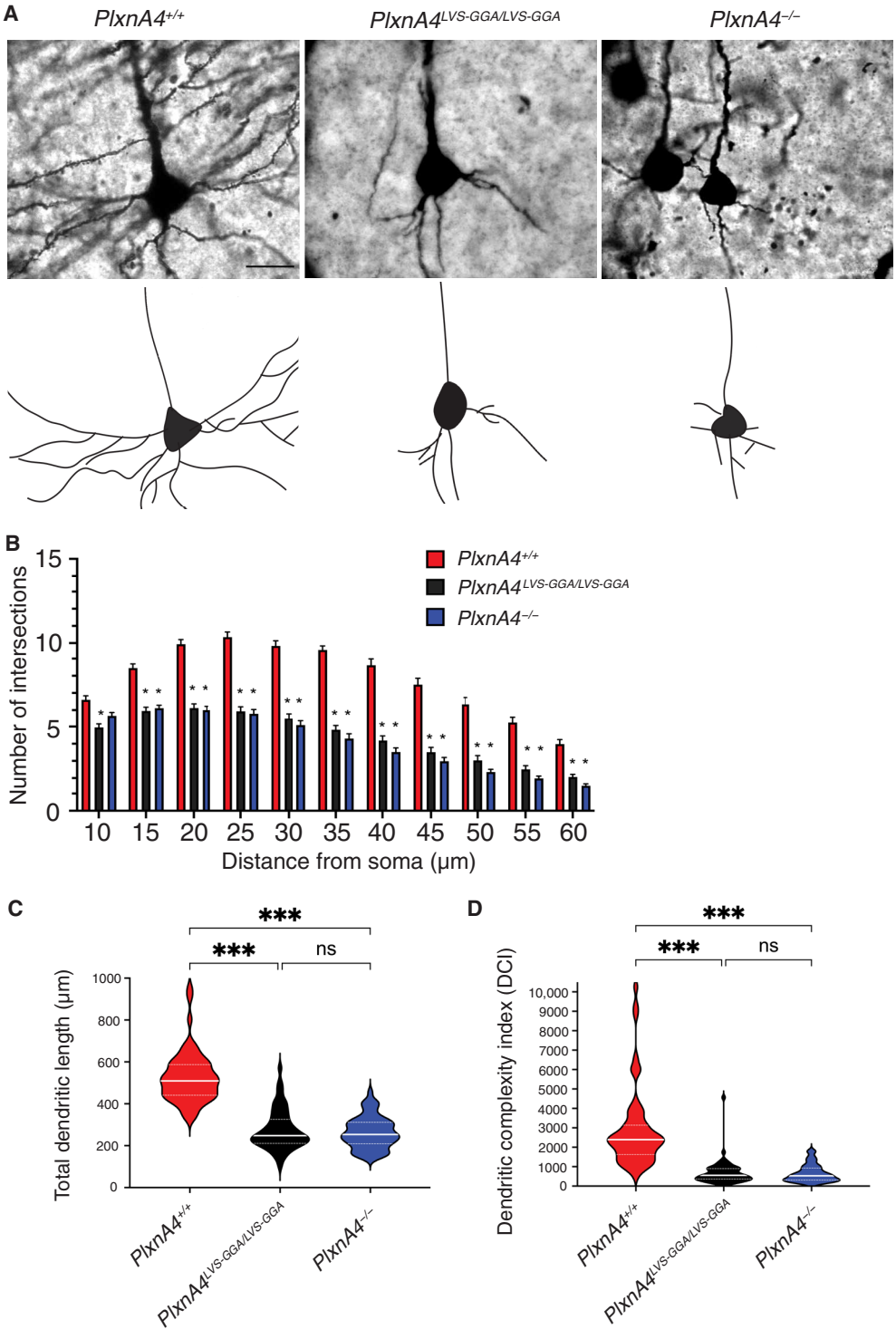

Fig. 2. The LVS motif in plexin-A4 is required for dendritic elaboration in cortical neurons in vivo. (**A**) Representative images and overlay tracings of Golgi-stained layer V cortical pyramidal neurons from the indicated mouse lines, analyzed in (B) to (D). Scale bar, 20 μm. (**B**) Sholl analysis of the number of dendritic intersections in layer V cortical pyramidal neurons from the indicated mouse lines. Data are means ± SEM from 20 neurons from each of $n = 3$ animals per genotype. $^{*}P < 0.001$ versus $PlxnA4^{+/+}$ by two-way ANOVA and Tukey's post hoc analysis. (**C** and **D**) Quantification of total dendritic length (C) and the dendritic complexity index (D) in layer V cortical pyramidal neurons from the indicated mouse lines. Data are means ± SEM from 20 neurons from each of $n = 3$ animals per genotype. $^{ns}P > 0.05$ (not significant) and $^{***}P < 0.001$ by one-way ANOVA and Tukey's post hoc analysis.

from the $PlxnA4^{LVS\text{-}GGA/LVS\text{-}GGA}$ neurons compared to the AP-alone treatment. Furthermore, the amount of Rnd1 pulled down from $PlxnA4^{-/-}$ neurons was significantly diminished for both AP-Sema3A and AP-alone treatments (Fig. 3, A and B). Therefore, we also confirmed the interaction between Rnd1 and plexin-A4 in cortical tissue lysates from postnatal day 5 (P5) pups, because the majority of dendritic growth in cortical neurons occurs during the first postnatal week (*40*, *41*). In P5 animals, mutant $PlxnA4^{LVS\text{-}GGA/LVS\text{-}GGA}$ receptors were still able to associate with Rnd1, but this association was significantly less (or weaker) compared with the WT $PlxnA4^{+/+}$ receptors, and little to no Rnd1 proteins were pulled down in the cortical lysate samples from the $PlxnA4^{-/-}$ animals (Fig. 3, C and D). These findings show that Rnd1 interacts with plexin-A4, in part by binding to the LVS motif, and Sema3A

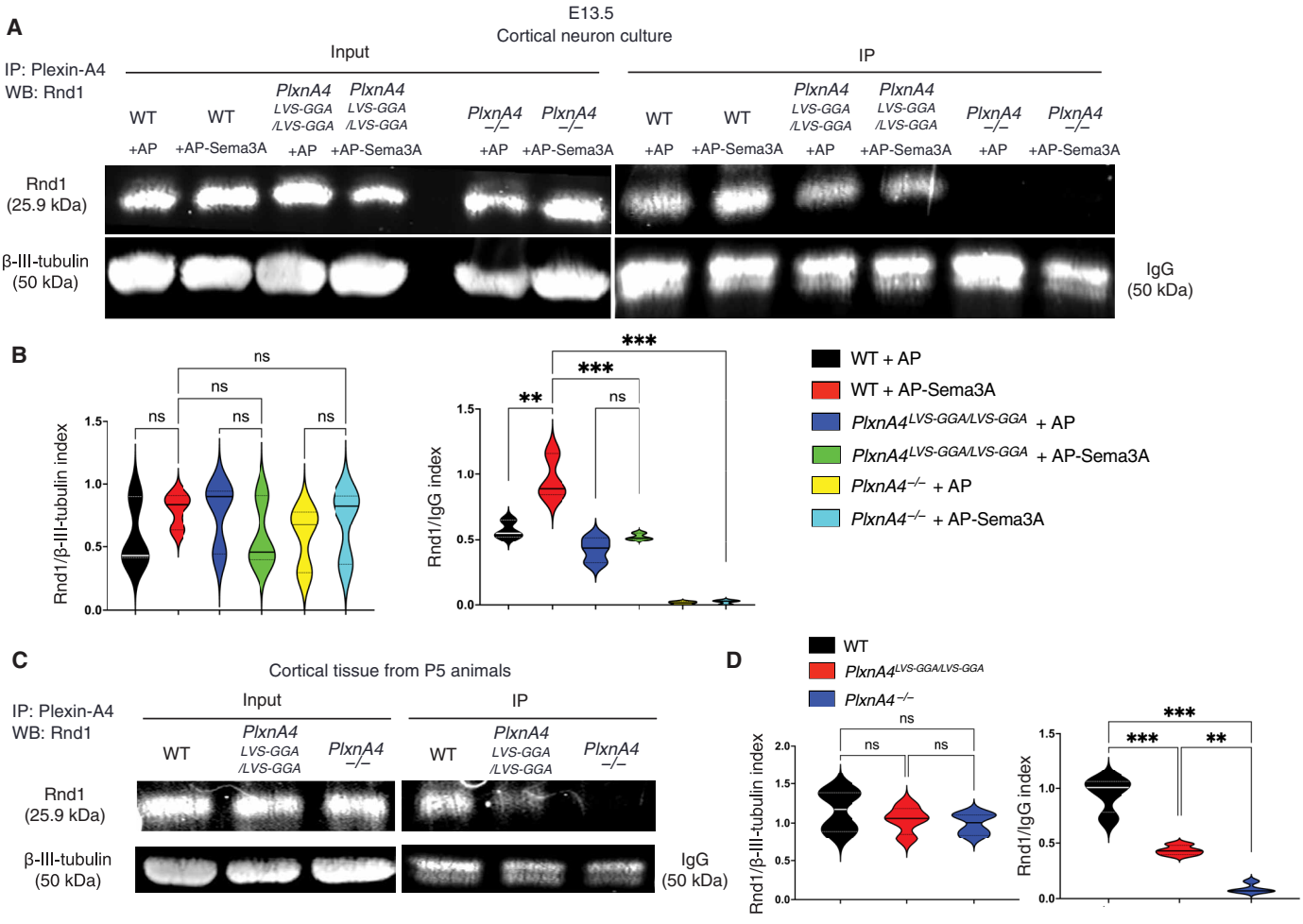

Fig. 3. Sema3A induces Rnd1 association with plexin-A4 through the LVS motif of the H/RBD cytoplasmic domain. (**A**) Western blotting (WB) analysis for Rnd1 and control proteins in lysates of E13.5 *PlxnA4*$^{+/+}$ (WT), *PlxnA4*$^{LVS\text{-}GGA/LVS\text{-}GGA}$, and *PlxnA4*$^{-/-}$ mouse cortical neurons treated with AP alone or AP-Sema3A for 15 min and immunoprecipitated with antibody to plexin-A4. Blots are representative of three independent experiments. (**B**) Quantification of the abundance of Rnd1 in blots described in (A) relative to that of β-III-tubulin and IgG. Data are means ± SEM from $n = 3$ independent cultures per condition. Color code in inset legend follows in sequence top to bottom as plots display left to right. $P > 0.05$ (ns, not significant), $^{***}P < 0.001$, and $^{**}P < 0.01$ by one-way ANOVA and Tukey's post hoc analysis. (**C** and **D**) Assay and analysis as described in (A) and (B), respectively, on cortical tissues from 5-day-old mice, $n = 4$ per condition.

activation of plexin-A4 increases this interaction in developing cortical neurons.

We next investigated the physiological role of Rnd1 in Sema3A-induced dendritic elaboration. Using our established primary cortical neuron cultures, we transfected *PlxnA4*$^{+/+}$ cortical neurons with either scrambled or *Rnd1*-targeted small interfering RNA (siRNA) and cultured neurons for 5 days. Cortical neurons were then stimulated with AP alone or AP-Sema3A (5 nM) for 24 hours to induce dendritic elaboration, and dendrites were immunostained with antibody to MAP2. Cortical neurons transfected with Rnd1 siRNA were unresponsive to Sema3A treatment in comparison with cortical neurons transfected with scrambled siRNA in elaborating dendrites (Fig. 4, A to C). Biochemical analysis confirmed the efficient and significant knockdown of Rnd1 in the cortical neuron cultures (Fig. 4D). Overall, these results show that Rnd1 associates with the Sema3A signaling receptor plexin-A4 through the LVS motif and is required for Sema3A-induced dendritic elaboration.

Sema3A/PlxnA4-mediated cortical dendrite elaboration requires RhoA inactivation downstream of the LVS motif signaling

Rnd1 promotes activity-dependent dendrite elaboration (*27*) and dendritic spine elongation in rat hippocampal neurons (*28*) by decreasing RhoA activity and its downstream effector, ROCK (*26*, *28*–*36*). Therefore, we examined whether inactivation of RhoA/ROCK signaling by Rnd1 is required for dendritic elaboration in response to Sema3A. We first examined whether RhoA activity is decreased in response to Sema3A in cortical neurons. Primary neurons were isolated from *PlxnA4*$^{LVS\text{-}GGA/LVS\text{-}GGA}$, *PlxnA4*$^{-/-}$, and *PlxnA4*$^{+/+}$ embryos, grown for 5 days in vitro (DIV), and were treated with either AP alone or AP-Sema3A for 15 min. Protein lysates were obtained and probed for RhoA–guanosine 5′-triphosphate (GTP) (active RhoA) and total RhoA in Western blot analysis. Sema3A treatment induced a decrease in RhoA-GTP levels compared with control treatment only in *PlxnA4*$^{+/+}$ cortical neurons (fig. S2, A and B). In contrast, Sema3A treatment did not induce RhoA inactivation in

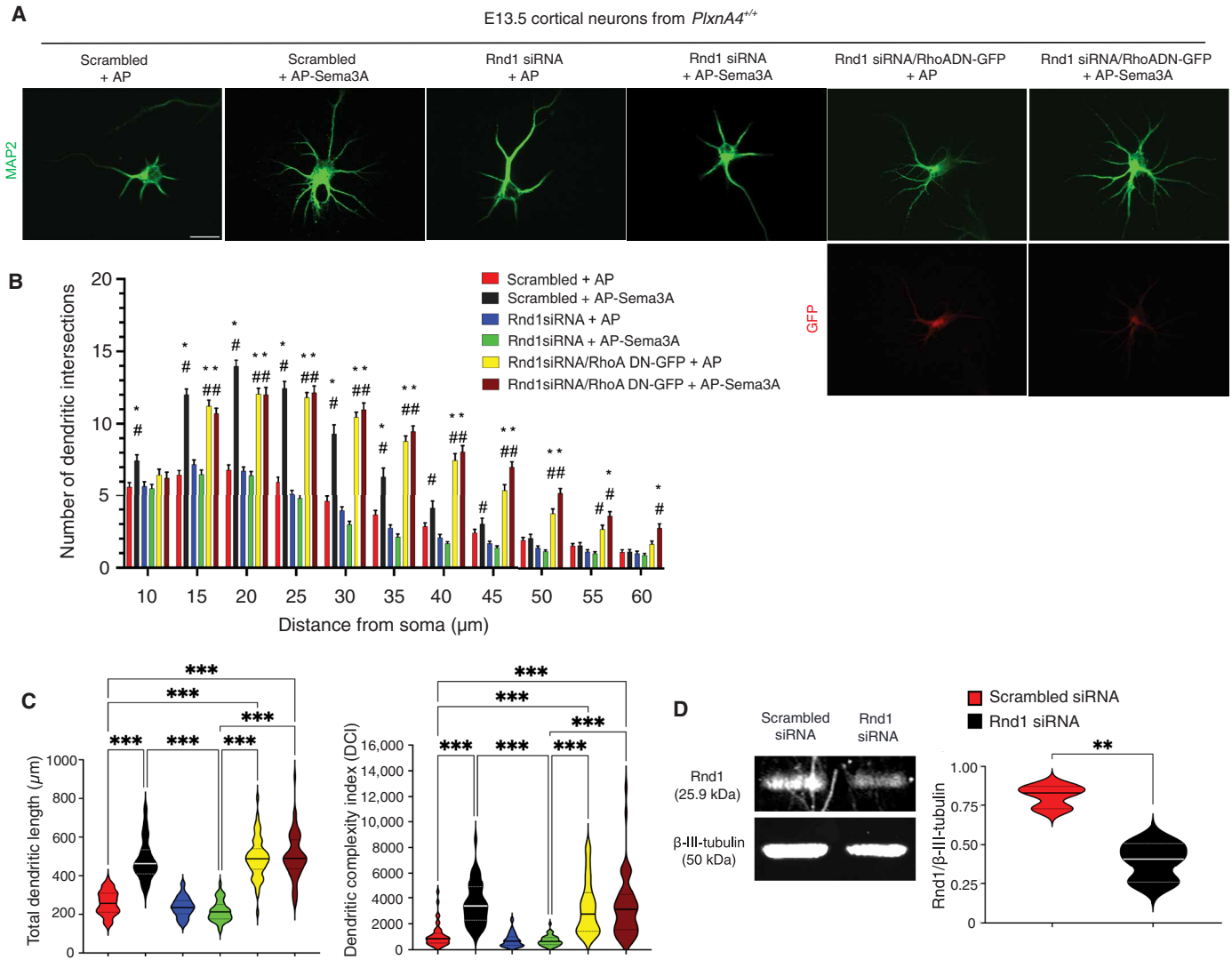

Fig. 4. The Rho GTPase Rnd1 and subsequent RhoA inactivation is necessary for Sema3A-induced dendritic elaboration in cortical neurons in vitro. (**A**) Representative images of E13.5 cortical neurons from *PlxnA4*$^{+/+}$ mice, transfected with Scrambled siRNA, Rnd1 siRNA, or Rnd1 siRNA + RhoADN-GFP (GFP dominant-negative RhoA) construct, then cultured for 5 days, treated with either AP alone or AP-Sema3A (5 nM) for 24 hours, and immunostained for the dendritic marker MAP2 (green) and, for the RhoADN-GFP transfected sets, GFP (red). Scale bar, 20 μm. (**B**) Sholl analysis representing the number of dendritic intersections under each condition of *PlxnA4*$^{+/+}$ cortical neurons. Data are means ± SEM from 15 neurons in each of $n = 3$ independent cultures per condition. Color code in inset legend follows in sequence top to bottom as bars display left to right. *$P < 0.001$ versus scrambled + AP and #$P < 0.001$ versus Rnd1 siRNA + Sema3A by two-way ANOVA with Tukey's post hoc test. (**C**) Total dendritic length and dendritic complexity index under each condition of *PlxnA4*$^{+/+}$ cortical neurons. Data are means ± SEM from 15 neurons from each of $n = 3$ independent cultures per condition. Color code follows that in (B), same sequence. ***$P < 0.001$ by one-way ANOVA Tukey's post hoc test. (**D**) Western blotting analysis and quantification of Rnd1 levels in E13.5 cortical neurons transfected in culture with scrambled or *Rnd1*-targeted siRNA. Data are means ± SEM for $n = 3$ independent cultures per condition. **$P < 0.01$ by Student's *t* test.

PlxnA4$^{LVS\text{-}GGA/LVS\text{-}GGA}$ or *PlxnA4*$^{-/-}$ neurons in response to Sema3A. To confirm the specificity of the RhoA-GTP antibody in our Western blot, we performed an IP using the RhoA-GTP antibody, then probed for total RhoA, and found that the IP RhoA(-GTP) did indeed decrease with AP-Sema3A in comparison with AP-alone treatment, consistent with our Western blotting analysis (fig. S2, C and D). Next, we tested the relationship between Rnd1 and RhoA activity in the context of Sema3A signaling. WT primary cortical neurons were transfected with either scrambled siRNA or Rnd1 siRNA, followed by AP-alone control or AP-Sema3A treatments. Our biochemical analysis showed that Sema3A treatment of control neurons (transfected with scrambled siRNA) resulted in lower levels of active RhoA as indicated by anti–RhoA-GTP densitometry compared with the AP-alone control treatment, whereas neurons transfected with Rnd1 siRNA without Sema3A treatment showed the highest level of active RhoA compared with all conditions (fig. S2, E and F). These results suggest that the Sema3A-induced decrease in RhoA activity is able to occur through another pathway in addition to the one mediated by Rnd1. We also examined whether RhoA inactivation occurs in vivo during dendritic development using cortical

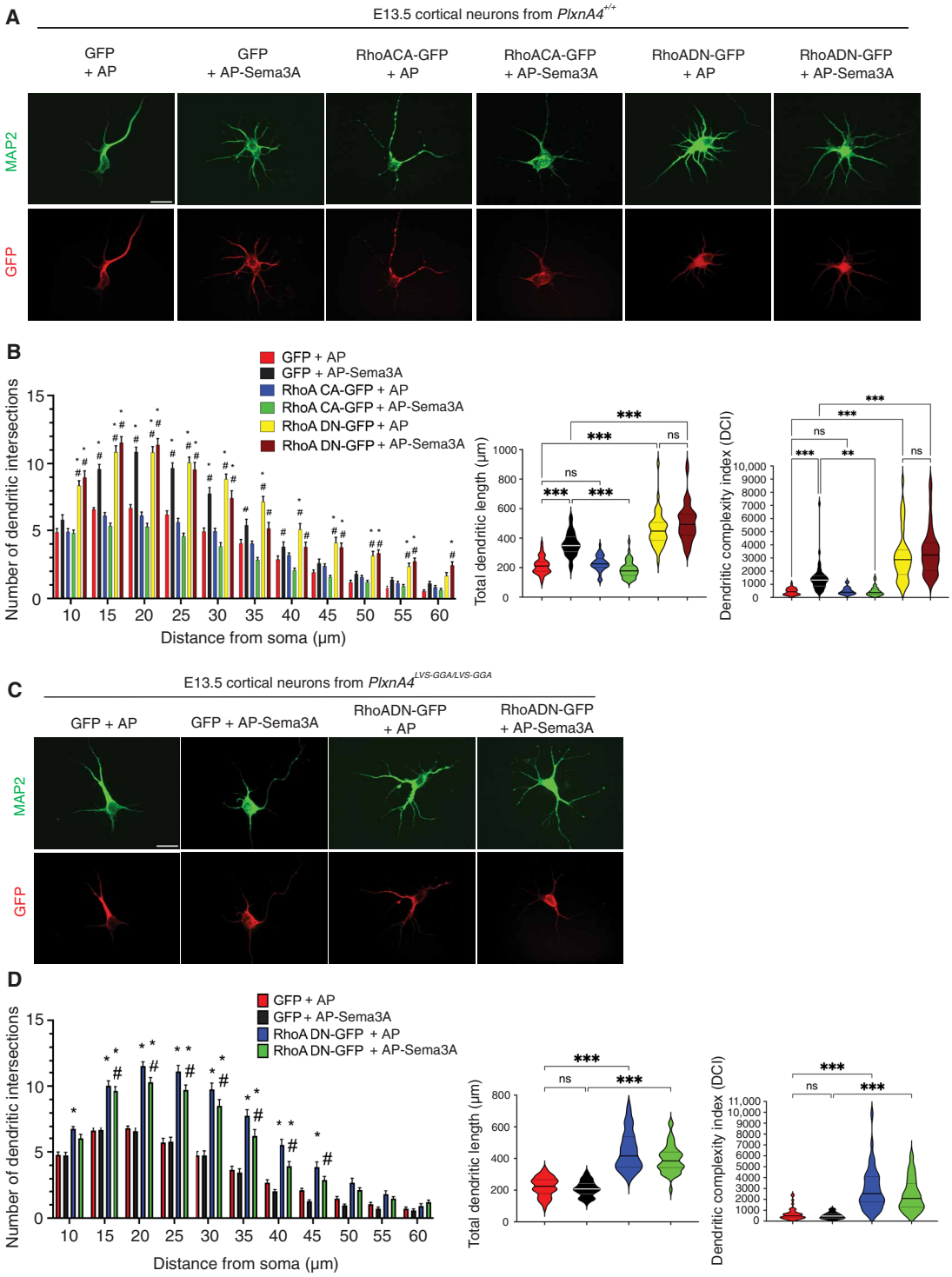

Fig. 5. Altered RhoA activity downstream of the LVS motif in plexin-A4 is seen with cortical dendritic elaboration in vitro. (**A**) Representative images of E13.5 cortical neurons from *PlxnA4*$^{+/+}$ mice, transfected with either GFP, constitutively active RhoA (RhoACA-GFP) or dominant-negative RhoA (RhoADN-GFP), cultured for 5 days, treated with either AP alone or AP-Sema3A (5 nM) for 24 hours, and immunostained for the dendritic marker MAP2 (green) and GFP (red). Scale bar, 20 μm. (**B**) Analysis of imaging described in (A) for the number of dendritic intersections (by Sholl analysis), total dendritic length, and dendritic complexity in E13.5 *PlxnA4*$^{+/+}$ cortical neurons transfected and treated as indicated. Data are means ± SEM from 15 neurons from each of $n = 3$ independent cultures per condition. Color code in inset legend follows in sequence top to bottom as bars and plots display left to right. For Sholl analysis, *$P < 0.001$ versus GFP + AP and #$P < 0.001$ versus RhoACA-GFP + Sema3A by two-way ANOVA and Tukey's post hoc analysis. For total dendritic length and DCI, ***$P < 0.001$ and **$P < 0.01$ by one-way ANOVA and Tukey's post hoc analysis ($^{ns}P > 0.05$, not significant). (**C** and **D**) As described and analyzed in (A) and (B), respectively, in E13.5 cortical neurons from *PlxnA4*$^{LVS\text{-}GGA/LVS\text{-}GGA}$ mice. Scale bar, 20 μm.

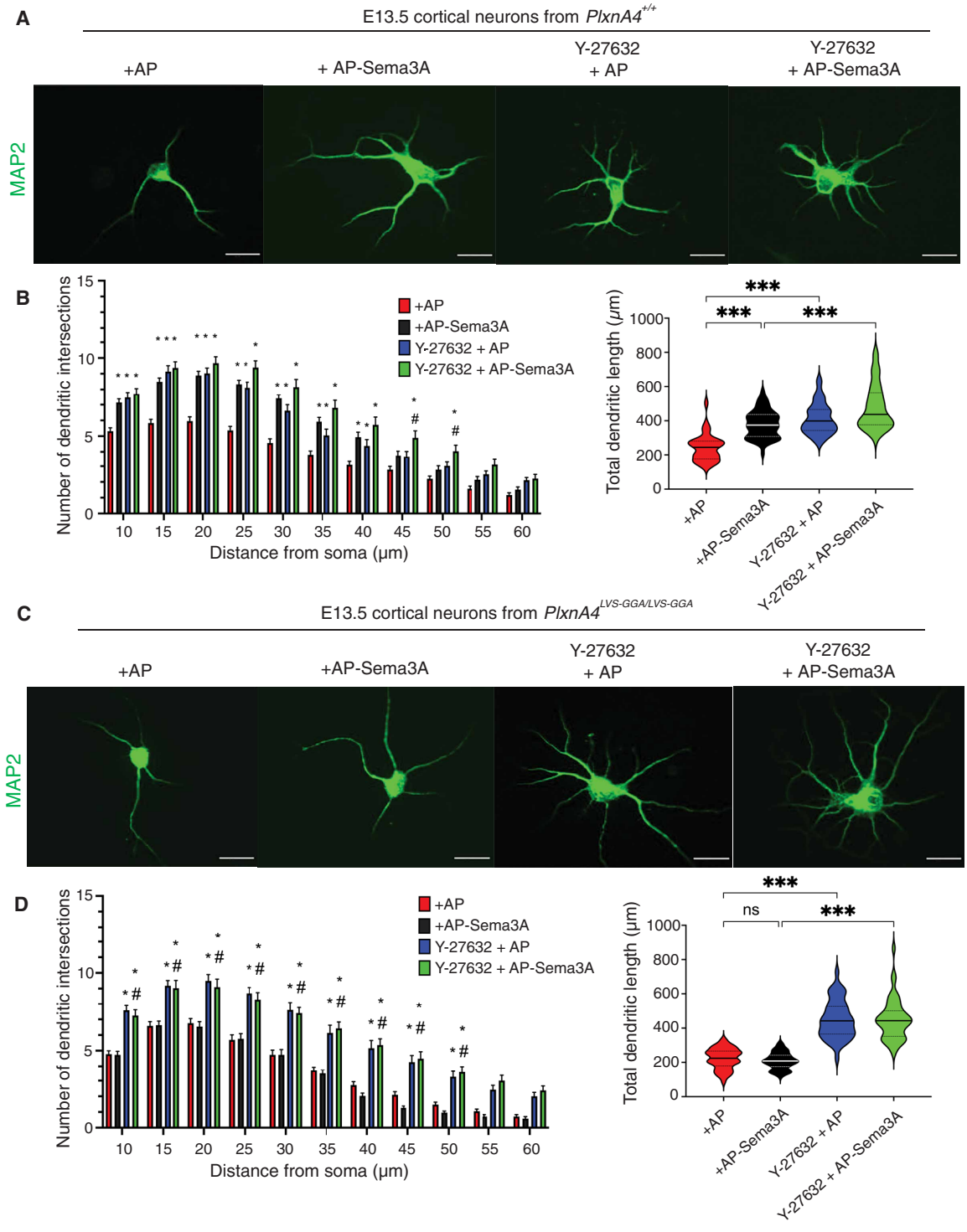

Fig. 6. ROCK inhibition downstream of the LVS motif in the plexin-A4 receptor is required for Sema3A-induced dendritic elaboration in cortical neurons in vitro. (**A**) Representative images of E13.5 cortical neurons from *PlxnA4*$^{+/+}$ mice cultured for 5 days; treated with AP alone, AP-Sema3A (5 nM), AP alone, or AP-Sema3A with ROCK inhibitor Y-27632 (10 μM) for 24 hours; and immunostained for the dendritic marker MAP2 (green). Scale bars, 20 μm. (**B**) Dendritic measurements (intersections and length) in the *PlxnA4*$^{+/+}$ neurons described in (A) for ROCK inhibitor experiment: Sholl analysis and total dendritic length in neurons. Data are means ± SEM from 15 neurons from each of $n = 3$ independent cultures per condition. Color code in inset legend follows in sequence top to bottom as bars and plots display left to right. For Sholl analysis, *$P < 0.001$ versus +AP and #$P < 0.033$ for Y-27632 + AP-Sema3A versus +AP-Sema3A by two-way ANOVA and Tukey's post hoc analysis. For total dendritic length, ***$P < 0.001$ by one-way ANOVA and Tukey's post hoc analysis. (**C** and **D**) Assays and analysis as described in (A) and (B), respectively, for E13.5 cortical neurons from *PlxnA4*$^{LVS\text{-}GGA/LVS\text{-}GGA}$ mice. Scale bars, 20 μm.

tissue lysates from P5 pups (*40*, *41*). In P5 animals, RhoA-GTP levels were significantly lower in *PlxnA4*$^{+/+}$ cortices compared with *PlxnA4*$^{LVS\text{-}GGA/LVS\text{-}GGA}$ and *PlxnA4*$^{-/-}$ cortices (fig. S2, G and H). These findings show that RhoA activity decreases in response to Sema3A, downstream of the LVS motif signaling in cortical neurons.

To test the physiological requirement of RhoA inactivation in Sema3A-mediated dendritic elaboration, we introduced constitutively active RhoA into *PlxnA4*$^{+/+}$ primary cortical neurons and quantified Sema3A-induced dendritic elaboration (Fig. 5, A and B). Our results indicate that the presence of constitutively active RhoA abolished dendritic elaboration in response to Sema3A in comparison with control–green fluorescent protein (GFP) transfected neurons treated with Sema3A (Fig. 5, A and B). In contrast, transfecting *PlxnA4*$^{+/+}$ cortical primary neurons (Fig. 5A), or *PlxnA4*$^{+/+}$ neurons transfected with Rnd1 siRNA (Fig. 4A), with a dominant negative RhoA construct induced even more dendritic branching and complexity regardless of the presence or absence of Sema3A compared with the control-GFP transfected neurons (Figs. 4, B and C, and 5C). These results indicate that RhoA activity suppresses dendritic branching and complexity. To investigate whether RhoA inactivation is mediated downstream of the LVS motif signaling, we transfected *PlxnA4*$^{LVS\text{-}GGA/LVS\text{-}GGA}$ cortical neurons with dominant negative RhoA and quantified their dendritic morphology. The introduction of dominant negative RhoA was able to rescue Sema3A-induced dendritic elaboration in comparison with control-GFP transfected *PlxnA4*$^{LVS\text{-}GGA/LVS\text{-}GGA}$ neurons treated with Sema3A (Fig. 5D). Collectively, our findings demonstrate that RhoA activity is decreased downstream of the Sema3A/plexin-A4(LVS)–Rnd1 signaling pathway and that this low level of RhoA activity is essential for Sema3A-induced cortical branching.

We also investigated whether ROCK is operating downstream of RhoA in Sema3A-mediated dendritic elaboration. In primary *PlxnA4*$^{+/+}$ cortical neurons treated with AP-Sema3A (5 nM) and the ROCK inhibitor (Y-27632; 10 μM) for 24 hours, these neurons were able to promote even more dendritic branching and growth compared with neurons treated with AP-Sema3A only (Fig. 6, A and B). We further examined whether the activity of ROCK is decreased downstream of the LVS motif signaling.

Our findings show that the inhibition of ROCK in *PlxnA4*$^{LVS\text{-}GGA/LVS\text{-}GGA}$ neurons rescued the dendritic phenotypes as compared with *PlxnA4*$^{LVS\text{-}GGA/LVS\text{-}GGA}$ neurons treated with AP-Sema3A or with AP-alone control condition (Fig. 6, C and D). This suggests that ROCK is inhibited downstream of the LVS motif in Sema3A/plexin-A4–induced cortical dendritic elaboration.

Balancing act between LVS-Rnd1-RhoA/ROCK and KRK-FARP2-Rac1 signaling

Pathways in cortical neuron dendrite elaboration

We previously showed that the KRK motif is required for Sema3A/plexin-A4–induced cortical neuron dendritic elaboration through FARP2-Rac1 signaling in vitro and in vivo (*16*). Here, we describe another pathway that is necessary for Sema3A/plexin-A4–induced dendritic elaboration through the LVS motif of the plexin-A4 receptor, which is required for GTPase binding and receptor activation (*19*, *23*, *38*). Therefore, we next asked whether there is interplay between the two signaling pathways to promote dendritic elaboration. To answer this question, we used our established cortical neuron culture system by transfecting *PlxnA4*$^{+/+}$ cortical neurons with constitutively active Rac1 and quantified Sema3A-induced dendritic elaboration. Our results indicate that the presence of constitutively active Rac1 promoted more dendritic elaboration, irrelevant of Sema3A treatment, in comparison with control-GFP transfected neurons (Fig. 7, A and B). We next asked whether constitutively active Rac1 is able to rescue the abrogated LVS-Rnd1-RhoA–mediated dendritic elaboration in *PlxnA4*$^{LVS\text{-}GGA/LVS\text{-}GGA}$ cortical neurons. We transfected *PlxnA4*$^{LVS\text{-}GGA/LVS\text{-}GGA}$ cortical neurons with constitutively active Rac1 and evaluated their dendritic morphology. The introduction of constitutively active Rac1 was able to rescue dendritic elaboration, with or without AP-Sema3A treatment, in comparison with control-GFP transfected *PlxnA4*$^{LVS\text{-}GGA/LVS\text{-}GGA}$ (Fig. 7, C and D). Together, our findings suggest cross-talk between LVS-Rnd1-RhoA and KRK-FARP2-Rac1 pathways underlying the Sema3A/plexin-A4 signaling mechanisms in promoting cortical neuron dendritic elaboration.

DISCUSSION

In this study, we characterized a signaling mechanism that is engaged downstream of Sema3A/plexin-A4 signaling to induce dendritic growth in developing mouse cortical neurons. In this mechanism, the LVS motif within the H/RBD domain of plexin-A4 mediated the receptor's association with and activation of the small GTPase Rnd1 and the repression of RhoA-ROCK signaling to promote dendritic elaboration. Thus, our results suggest cross-talk between two GTPase-mediated signaling pathways downstream of plexin-A4: FARP2-Rac1 (*11*, *16*) and Rnd1-RhoA-ROCK (Fig. 8, A and B) in promoting dendritic elaboration during cortical neuron development.

Given that both Rnd1 and RhoA are Rho GTPases, Rnd1 is unlikely to directly decrease RhoA activity. Several molecules have the potential to act downstream of Rnd1 in the Sema3A-Nrp1/plexin-A4 signaling pathway in developing neurons. One study using fibroblasts reported that Rnd1 decreases RhoA activity through the activation of p190 RhoGAP, a negative regulator of RhoA, resulting in the extension of cellular processes (*35*). This cellular effect is also seen in response to other Rnd1-interacting proteins: socius in fibroblasts (*31*) and the heat shock protein 70 (Hsp70)/Hsp90 cochaperone stress–inducible protein-1 (*42*) in fibroblasts and PC-12 cells (*43*). Moreover, the microtubule regulator SCG10 (superior cervical ganglia neural–specific 10 protein) exhibits binding specificity to Rnd1 and promotes Rnd1-induced axonal extension in hippocampal neurons (*44*). The related Ras GTPase protein family member R-Ras has previously been shown to promote the association of Rnd1 with plexin-A1 (*15*) and plexin-B1 (*21*) to induce plexin GAP activity (*21*, *45*). Another closely related family member to R-Ras, M-Ras, is a potential molecule downstream of Rnd1 in dendrite development (*46*). M-Ras is highly abundant in the central nervous system, particularly in the cortex and hippocampus (*47*, *48*), and promotes dendritic arborization by activating the extracellular signal–regulated kinase pathway through B-Raf and lamellipodin in cortical neurons (*47*–*50*) and PC-12 cells (*47*, *51*).

Other mechanisms could also be involved. In Sema6A-induced plexin-A4–mediated dendritic growth of motor neurons in the vertebrate spinal cord, RhoGEF FARP1 is an effector that promotes dendritic growth by regulating RhoA GTPase activity (*52*). Rnd3, a closely related homolog of Rnd1, interacts with ROCK1 to inhibit it from promoting stress fiber assembly in non-neuronal cells (*53*). A much-needed future study would be to evaluate whether these

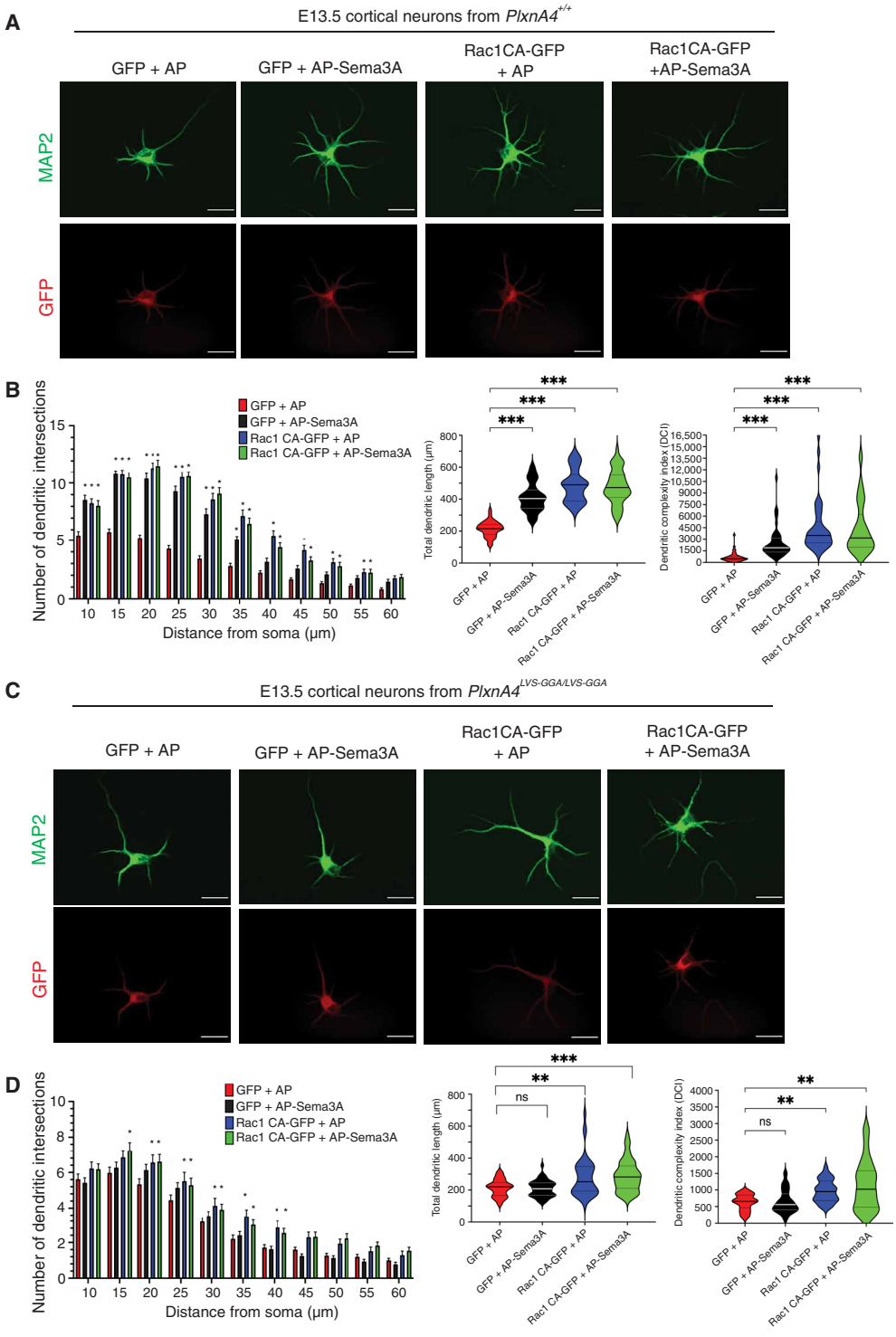

Fig. 7. RhoA and Rac1 interact downstream of Sema3A/plexin-A4 signaling in primary cortical neuron dendritic elaboration. (**A**) Representative images of E13.5 cortical neurons from *PlxnA4*$^{+/+}$ mice, transfected with either GFP or constitutively active Rac1 (Rac1CA-GFP), cultured for 5 days, then treated with either AP alone or AP-Sema3A (5 nM) for 24 hours, and immunostained for the dendritic marker MAP2 (green) and GFP (red). Scale bars, 20 μm. (**B**) Dendritic measurements in the *PlxnA4*$^{+/+}$ neurons described in (A). Data are means ± SEM from 15 neurons from each of $n = 3$ independent cultures per condition. For Sholl analysis, $^{*}P < 0.001$ versus GFP + AP by two-way ANOVA and Tukey's post hoc analysis. For total dendritic length and DCI, $^{***}P < 0.001$ and $^{**}P < 0.01$ by one-way ANOVA and Tukey's post hoc test. (**C** and **D**) Assays and analysis as described in (A) and (B), respectively, in E13.5 cortical neurons from *PlxnA4*$^{LVS\text{-}GGA/LVS\text{-}GGA}$ mice. Scale bars, 20 μm. For Sholl analysis, $^{*}P < 0.033$ versus GFP + AP by two-way ANOVA and Tukey's post hoc analysis. In total dendritic length and DCI, as in (B), $^{**}P < 0.01$ and $P > 0.05$ (ns, not significant) by one-way ANOVA and Tukey's post hoc test.

potential molecules are indeed downstream of the plexin-A4–LVS/Rnd1 pathway in cortical neurons to promote dendritic elaboration.

Previous findings from our group described a pathway of dendritic elaboration downstream of the KRK motif of plexin-A4 through FARP2-Rac1 signaling that is dispensable in Sema3A/plexin-A4–mediated axon guidance events (*16*). Our current findings uncovered another signaling pathway downstream of the LVS motif of the plexin-A4 receptor through its associations with Rnd1, which led to RhoA inactivation to enable dendritic elaboration in the same cortical neurons during development. Clues from previous studies suggested a number of potential cross-talk mechanisms. Early evidence showed that Rnd1 promotes neurite formation through regulating Rac1 activity in PC-12 cells (*54*). This is further supported by the finding that upon Sema3A activation, Rac1 binds the Rho GTPase

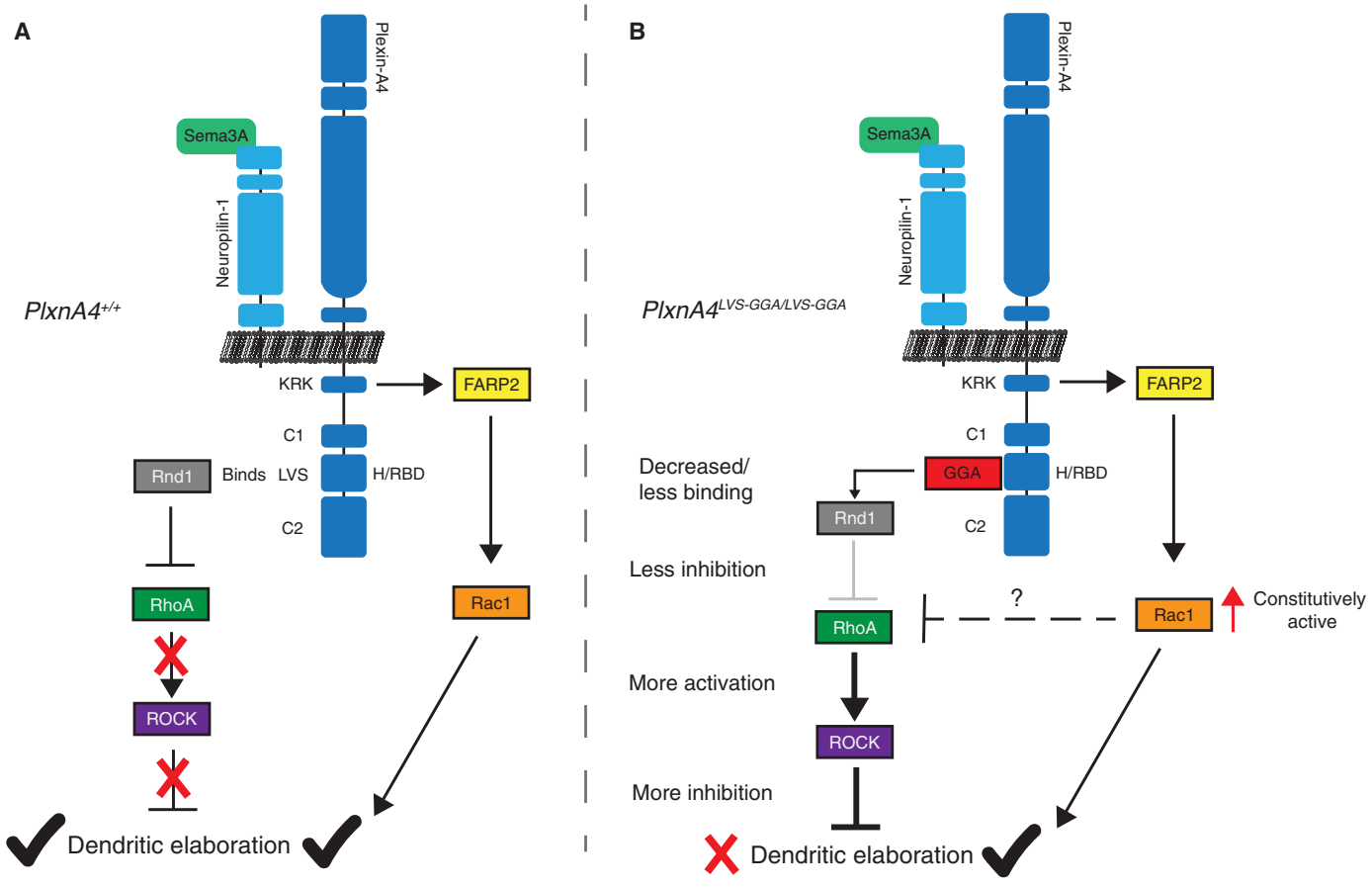

Fig. 8. A working model for Sema3A-Nrp1/plexin-A4–induced dendritic elaboration in cortical neurons. (**A**) Sema3A binds to its holoreceptor complex Nrp1/PlxnA4, inducing the binding of Rnd1 to PlxnA4 receptor at the LVS motif. This induces the inactivation of RhoA GTPase, a negative regulator of dendritic elaboration and its downstream effector ROCK, promoting dendritic elaboration. (**B**) Substitution of LVS to GGA attenuates the binding of Rnd1 to PlxnA4 receptor causing RhoA to remain activated and increase recruitment of ROCK, which, in turn, inhibits dendritic elaboration. The activation of Rac1 signaling rescued the dendritic elaboration phenotype in *PlxnA4*$^{LVS\text{-}GGA/LVS\text{-}GGA}$ cortical neurons, suggesting cross-talk between the LVS-Rnd1-RhoA and KRK-FARP2-Rac1 pathways.

binding domain (H/RBD) of plexin-A1, which contains this LVS motif that is conserved in all type A plexins. This interaction further increased the levels of active Rac1, suggesting a positive feedback loop in this signaling pathway (*23*, *45*). Moreover, one model suggested that Rnd1 and Rac1 exhibit sequential binding to the plexin H/RBD cytoplasmic domain (*55*); the constitutively active Rnd1 binds the H/RBD domain to release the autoinhibitory folding of the plexin cytoplasmic domains, which then allows active Rac1 to bind to the H/RBD domain (*23*). This model suggests that the binding site on the plexin-A4 receptor for Rac1 may also be the LVS motif, which supports our findings because it appears that endogenous Rac1 was not able to suppress the dendritic phenotypes in the *PlxnA4*$^{LVS\text{-}GGA/LVS\text{-}GGA}$–mutant cortical neurons after Sema3A stimulation. However, the overexpression of a constitutively active Rac1 was able to rescue the dendritic phenotype in the same neurons, supporting the idea that Rac1 activation and/or binding to plexin-A4 was abolished because of the switch of the LVS to GGA. Future experiments will test whether Rac1 and RhoA compete for interaction with plexin-A4 at the LVS motif.

Our study demonstrated that the conserved LVS motif in the cytoplasmic domain of the guidance receptor plexin-A4 is sufficient to promote dendrite growth and branching in developing mouse cortical neurons. Upon activation by its specific ligand Sema3A, the LVS motif in plexin-A4 binds to the small GTPase Rnd1, which leads to the inhibition of another small GTPase RhoA; this promotes dendritic elaboration, mostly likely through the reorganization of the cytoskeleton. These findings provide new insights into the multifunctional Sema3A/plexin-A4 signaling pathways that orchestrate the proper elaboration of neuronal morphologies and neuronal wiring during nervous system development.

MATERIALS AND METHODS

Animals

For all animals, E0.5 was determined as the day that the vaginal plug was observed. Pups were weaned at P21 and kept on a 12-hour light/12-hour dark cycle at controlled temperature with food and water ad libitum. All animal work in this study was approved by the Institutional Animal Care and Use Committees Rutgers University Newark.

PlxnA4$^{LVS\text{-}GGA/LVS\text{-}GGA}$ mice were generated by introducing point mutations in the cytoplasmic LVS motif of the plexin-A4 receptor at

the Rutgers Cancer Institute of New Jersey Genome Editing Shared Resource (P30CA072720-5922). Using the CRISPR-Cas9 system, *PlxnA4* L1596, V1597, and S1598 in exon 27 were changed to GGA. CRISPR guide RNA (GGTACCAGATGGTTCTGTGG) (MilliporeSigma) complexed with Cas9 protein (MilliporeSigma) was microinjected with SSODN donor [Integrated DNA Technologies (IDT)] sequence 5′-TGACCACACCTGCTTTGGATGCTTCTACTTCCCACCCCT TACACCTGATGAGATCTTACCATATTTACTTGCT-GAAGTCCTGGAGACAGTGGAGTTGTTCACTGCATTGTAG-GCTGTCACTTGCTTGGcCcCTccAGCgACCACAGAAC-CATCTGGTACCTAGGGGAAAGGTTTCTAAGA-3′ [lower case are mutations to put in the glycines and change the protospacer adjacent motif (PAM)] into C57BL/6J zygotes. Founders were obtained after screening with HaeIII (NEB) digest (underlined in donor SSODN) and were then bred to C57BL/6J. The specificity of the desired mutation was confirmed using Sanger sequencing (Fig. 1A) and tail tip genomic DNA PCR genotyping (Fig. 1B). In PCR genotyping, primers *PlxnA4A* (5′-AAGGTGCTAATTGTCCCTCACTGC-3′) and *PlxnA4B* (5′-GGTCAGCTGACCTGATCCTCTATC-3′) were used, followed by HaeIII restriction digest.

PlxnA4$^{-/-}$ mice were previously generated as described (*13*). E13.5 embryo cortices were dissected, and cortical pyramidal neurons were cultured as described in the methods below.

Primary neuronal cultures

Cortical neurons were dissected from E13.5 *PlxnA4*$^{LVS\text{-}GGA/LVS\text{-}GGA}$, *PlxnA4*$^{-/-}$, and *PlxnA4*$^{+/+}$ mice as described in our previous studies (*11*, *16*). Before plating *PlxnA4*$^{LVS\text{-}GGA/LVS\text{-}GGA}$ and *PlxnA4*$^{+/+}$ neurons, dissociated neurons were transfected with Rnd1 siRNA (Dharmacon, M-055272-01-0005), scrambled siRNA (Dharmacon, #D-001206-13-05), constitutively active RhoA plasmid (Addgene, #12968), dominant negative RhoA plasmid (Addgene, #12960), constitutively active Rac1 plasmid (Addgene, #12981), or pmaxGFP vector (Lonza, #VPG-1001) using the Amaxa Mouse Neuron Nucleofector Kit (Lonza, #VPG-1001). In addition, some primary neuronal cultures were treated with the ROCK inhibitor Y-27632 (10 μM; Abcam, #ab120129) (*56*). Neurons were then seeded at a density of ~11,000 cells/cm^2 on glass coverslips (coated with poly-D-lysine, 0.1 mg/ml; #P6407) in 12-well plates (TPP, #92412) or in poly-D-lysine–coated six-well plates. Neurons were grown in neurobasal growth medium supplemented with 2% B-27 (Gibco, #17504-044), 1% penicillin-streptomycin (Gibco, #15140122), and 1% GlutaMAX (Gibco, #35050) for 5 DIV. On DIV 5, *PlxnA4*$^{LVS\text{-}GGA/LVS\text{-}GGA}$ and *PlxnA4*$^{+/+}$ cortical neuronal cultures were treated with 5 nM of either AP-Sema3A or AP-only ligands for 24 hours before processing for immunocytochemistry, co-IP, or Western blotting.

AP-Sema3A production

Human embryonic kidney (HEK) 293T cells (American Type Culture Collection, #CRL-3216) were used to generate AP-tagged Sema3A (AP-Sema3A) or AP alone as established earlier (*11*, *16*). HEK293T cells were grown in Dulbecco's modified Eagle medium containing 10% fetal bovine serum (VWR, #97068-085) and 1% penicillin-streptomycin. HEK293T cells were transfected with an AP-alone or AP-Sema3A plasmid (*57*) using BioT (Bioland Scientific, #B01-01). The secreted AP alone or AP-Sema3A in the medium was collected in Amicon ultra-15 UFC (MilliporeSigma, #910024). AP alone or AP-Sema3A concentration was measured using AP activity assay (*11*, *16*).

Immunocytochemistry

To examine cortical neuron dendritic morphology, cortical neurons were fixed with 4% paraformaldehyde and processed for immunocytochemistry as established before (*11*, *16*). The following primary antibodies were used (table S1): polyclonal rabbit anti-MAP2 (1:1000; Cell Signaling Technology, catalog no. 4542S) and monoclonal mouse anti-GFP (1:1000; lnvitrogen, catalog no. A-11120). Secondary antibodies were as follows: Alexa Fluor 488 donkey anti-rabbit immunoglobulin G (1:500; Thermo Fisher Scientific, catalog no. A-21206) and Cy3 donkey anti-mouse (1:500; Jackson lmmunoResearch, catalog no. 715-165-150). After immunostaining, coverslips were fixed on microscope slides using mounting medium (Mowiol, MilliporeSigma, #81381)/10% *p*-phenylenediamine (Sigma-Aldrich, catalog no. 78460). For cell surface expression of *PlxnA4*$^{LVS\text{-}GGA/LVS\text{-}GGA}$ and *PlxnA4*$^{+/+}$ proteins, primary cortical neurons were immunostained without Triton permeabilization.

Golgi staining

Whole-brain tissue from adult mice (2 to 3 months old) from different genotypes, males and females, was dissected out and preprocessed for Golgi staining as per the kit manufacturer's instructions (FD Rapid GolgiStain Kit, FD NeuroTechnologies, #PK401). Brain tissues were then embedded in optimal cutting temperature (OCT) embedding solution (Tissue-Tek, catalog no. 4583) and sectioned into 100-μm sagittal sections using a cryostat and mounted onto microscope slides. Golgi staining protocol provided by the kit manufacturer was followed exactly.

Western blotting

Cortices from *PlxnA4*$^{LVS\text{-}GGA/LVS\text{-}GGA}$, *PlxnA4*$^{-/-}$, and *PlxnA4*$^{+/+}$ P5 pups, both males and females, or E13.5 cultured primary cortical neurons were lysed in modified radioimmunoprecipitation assay (RIPA) buffer [1× tris-buffered saline (TBS), 10% glycerol, 1% Triton X-100, and 1% NP40, protease inhibitors (Roche cOmplete, #11697498001)] and then centrifuged at 14,000*g* for 10 min. Protein levels were quantified using Bradford assay (*58*), and protein samples were eluted in 4× Laemmli buffer. Samples were loaded into a 10% polyacrylamide gel for SDS–polyacrylamide gel electrophoresis, were run to resolve proteins, and then were transferred onto nitrocellulose membranes (Bio-Rad, #1620097). Membranes were then incubated in 5% blocking solution in TBS-Tween for 1 hour at room temperature. Membranes were kept in the desired primary antibody solution overnight at 4°C with one of the following antibodies (table S1): anti–plexin-A4 rabbit polyclonal antibody (Cell Signaling Technology, #C5D1), anti-Rnd1 mouse monoclonal antibody (1:2000; OriGene Technologies, #TA501691), anti–β-tubulin rabbit antibody (1:5000; Cell Signaling Technology, #5568), anti-Nrp1 goat antibody (1:1000; R&D Systems, #AF566), anti–RhoA-GTP mouse monoclonal antibody (1:1000; NewEast Biosciences, #26904), or anti-RhoA rabbit polyclonal antibody (1:1000; Abcam, #Ab68826). The anti–RhoA-GTP antibody was validated for Western blot to specifically detect active RhoA(-GTP) on a Western blot in a previous study (*59*). Membranes were washed three times for 10 min each and then incubated in secondary antibodies (anti-mouse IRDye 680RD donkey anti-mouse IgG (1:10,000; LI-COR, #926-68072) and IRDye 800CW donkey anti-rabbit IgG (1:10,000; LI-COR, #926-32213). Membranes were scanned using a LI-COR scanner, and images were analyzed using ImageJ.

Coimmunoprecipitation

Cortices from *PlxnA4*$^{LVS\text{-}GGA/LVS\text{-}GGA}$, *PlxnA4*$^{-/-}$, and *PlxnA4*$^{+/+}$ pups at P5 or E13.5 cultured primary cortical neurons were lysed in modified RIPA buffer (1× TBS, 10% glycerol, 1% Triton X-100, and 1% NP40, protease inhibitors) and then centrifuged at 14,000*g* for 10 min. Protein levels were quantified using the Bradford assay, and 500 μg of total protein underwent preclearing with Protein G Sepharose 4 Fast Flow (GE Healthcare, #GE17-0618-01) for 2 hours at 4°C on a rotor. After centrifugation at 14,000*g* for 7 min, supernatants were incubated with anti–plexin-A4 antibody (Cell Signaling Technology, #C5D1; table S1) or anti-Nrp1 goat antibody (R&D Systems, #AF566) at 4°C on a rotor overnight. Fifty microliters of Protein G Sepharose 4 Fast Flow was incubated with the lysates for 4 hours at 4°C on a rotor. Immunoprecipitates were washed three times with ice-cold modified RIPA buffer, extracted in 2× Laemmli buffer, and processed for Western blotting. Membranes were incubated with rabbit polyclonal anti–plexin-A4 antibody (Cell Signaling Technology, #C5D1), anti-Rnd1 mouse monoclonal antibody (1:2000; OriGene Technologies, #TA501691), and rabbit anti–β-tubulin antibody (1:5000; Cell Signaling Technology, #5568). As a protein loading control, membranes were initially probed with the secondary antibody anti-rabbit (primary antibody from rabbit). We acknowledge that using the total levels of plexin-A4 input as the reference control would have been better practice and more definitive than normalizing to the IgG. Unfortunately, because of unforeseen circumstances around the pandemic, the depleted mouse resources did not make it possible to correct this after the fact.

Microscopy and photodocumentation

Z-stack confocal micrographs were obtained from Golgi-stained brain sections or immunofluorescence-stained primary cortical neurons on glass coverslips. An Axio Examiner Z1 upright microscope with a Yokogawa spinning disk (Carl Zeiss) and an oil immersion 63× (numerical aperture 1.4) objective (PlanApo, Carl Zeiss) were used to obtain the images. *Z*-stacks projections were generated for each neuron and used for dendritic morphology analysis. Images were used to trace dendritic arbors in each neuron in grayscale mode using Adobe Photoshop for quantifications.

Dendritic arbor quantifications

Sholl analysis quantifies the complexity of dendritic trees by plotting the number of dendritic intersections against the radial distance from the center of the soma (*60*). The National Institutes of Health ImageJ and Sholl Analysis Plugin were used to perform Sholl analysis. Sholl analysis parameters were set as the following: The radial distance started from 10 to 60 μm, and the interval between different distances was 5 μm.

Total dendritic length was acquired using NeuronJ plugin on ImageJ software (*61*). DCI is a quantitative representation of the complexity of the dendritic arbor based on branch tip orders, number of branch tips, total arbor length, and number of primary dendrites (*62*). The DCI was calculated using the following equation:

$$\mathrm{DCI} = \frac{\sum \text{branch tip orders} + \#\ \text{of branch tips}}{(\#\ \text{of primary dendrites}) \times (\text{total dendrite length})}$$

Statistical analysis

For the plexin-A4 protein levels experiment, five animals of each genotype were analyzed, and statistical analysis was performed using one-way analysis of variance (ANOVA) and Tukey's post hoc analysis ($P < 0.001$). In Golgi-stained layer V cortical pyramidal neurons, three animals per genotype were analyzed. In cortical neuronal cultures, three or four independent cultures were performed per experimental condition where each culture represents cortices taken from embryos from one-timed pregnant female mouse. For dendritic arbor quantifications, two-way ANOVA with Tukey's post hoc analysis was used in Sholl analysis, whereas one-way ANOVA with Tukey's post hoc analysis was used in total dendritic length and DCI (*P* values are indicated in each figure). For co-IP experiments, three cultures per genotype in vitro and four animals per genotype in vivo were analyzed. Statistical analysis was done using one-way ANOVA and Tukey's post hoc analysis (*P* values are indicated on each figure). For Rnd1 siRNA knockdown protein levels experiment, three cultures per condition were included and analyzed using Student's *t* test ($P < 0.01$). For RhoA activity experiments, statistical analysis was done using one-way ANOVA and Tukey's post hoc analysis (*P* values are indicated on each figure). GraphPad Prism was used for statistical analyses of the different experiments.

Supplementary Materials

This PDF file includes:

Figs. S1 and S2
Table S1

Other Supplementary Material for this manuscript includes the following:

MDAR Reproducibility Checklist

REFERENCES AND NOTES

1. D. J. Solecki, E.-E. Govek, T. Tomoda, M. E. Hatten, Neuronal polarity in CNS development. *Genes Dev.* **20**, 2639–2647 (2006).
2. S. E. Newey, V. Velamoor, E.-E. Govek, L. Van Aelst, Rho GTPases, dendritic structure, and mental retardation. *J. Neurobiol.* **64**, 58–74 (2005).
3. M. B. Ramocki, H. Y. Zoghbi, Failure of neuronal homeostasis results in common neuropsychiatric phenotypes. *Nature* **455**, 912–918 (2008).
4. F. C. de Anda, A. L. Rosario, O. Durak, T. Tran, J. Gräff, K. Meletis, D. Rei, T. Soda, R. Madabhushi, D. D. Ginty, A. L. Kolodkin, L.-H. Tsai, Autism spectrum disorder susceptibility gene TAOK2 affects basal dendrite formation in the neocortex. *Nat. Neurosci.* **15**, 1022–1031 (2012).
5. C. E. Moyer, M. A. Shelton, R. A. Sweet, Dendritic spine alterations in schizophrenia. *Neurosci. Lett.* **601**, 46–53 (2015).
6. M. Nishimura, X. Gu, J. W. Swann, Seizures in early life suppress hippocampal dendrite growth while impairing spatial learning. *Neurobiol. Dis.* **44**, 205–214 (2011).
7. A. B. Huber, A. L. Kolodkin, D. D. Ginty, J.-F. Cloutier, Signaling at the growth cone: Ligand-receptor complexes and the control of axon growth and guidance. *Annu. Rev. Neurosci.* **26**, 509–563 (2003).
8. A. L. Kolodkin, M. Tessier-Lavigne, Mechanisms and molecules of neuronal wiring: A primer. *Cold Spring Harb. Perspect. Biol.* **3**, a001727 (2011).
9. V. Fenstermaker, Y. Chen, A. Ghosh, R. Yuste, Regulation of dendritic length and branching by semaphorin 3A. *J. Neurobiol.* **58**, 403–412 (2004).
10. C. Gu, E. R. Rodriguez, D. V. Reimert, T. Shu, B. Fritzsch, L. J. Richards, A. L. Kolodkin, D. D. Ginty, Neuropilin-1 conveys semaphorin and VEGF signaling during neural and cardiovascular development. *Dev. Cell* **5**, 45–57 (2003).
11. G. Mlechkovich, S.-S. Peng, V. Shacham, E. Martinez, I. Gokhman, A. Minis, T. S. Tran, A. Yaron, Distinct cytoplasmic domains in Plexin-A4 mediate diverse responses to semaphorin 3A in developing mammalian neurons. *Sci. Signal.* **7**, ra24 (2014).
12. T. S. Tran, M. E. Rubio, R. L. Clem, D. Johnson, L. Case, M. Tessier-Lavigne, R. L. Huganir, D. D. Ginty, A. L. Kolodkin, Secreted semaphorins control spine distribution and morphogenesis in the postnatal CNS. *Nature* **462**, 1065–1069 (2009).
13. A. Yaron, P.-H. Huang, H.-J. Cheng, M. Tessier-Lavigne, Differential requirement for Plexin-A3 and -A4 in mediating responses of sensory and sympathetic neurons to distinct class 3 semaphorins. *Neuron* **45**, 513–523 (2005).
14. J. W. Legg, C. M. Isacke, Identification and functional analysis of the ezrin-binding site in the hyaluronan receptor, CD44. *Curr. Biol.* **8**, 705–708 (1998).

15. T. Toyofuku, J. Yoshida, T. Sugimoto, H. Zhang, A. Kumanogoh, M. Hori, H. Kikutani, FARP2 triggers signals for Sema3A-mediated axonal repulsion. *Nat. Neurosci.* **8**, 1712–1719 (2005).
16. V. Danelon, R. Goldner, E. Martinez, I. Gokhman, K. Wang, A. Yaron, T. S. Tran, Modular and distinct Plexin-A4/FARP2/Rac1 signaling controls dendrite morphogenesis. *J. Neurosci.* **40**, 5413–5430 (2020).
17. M. H. Driessens, H. Hu, C. D. Nobes, A. Self, I. Jordens, C. S. Goodman, A. Hall, Plexin-B semaphorin receptors interact directly with active Rac and regulate the actin cytoskeleton by activating rho. *Curr. Biol.* **11**, 339–344 (2001).
18. Y. Tong, M. Buck, ^{1}H, ^{15}N and ^{13}C resonance assignments and secondary structure determination reveal that the minimal Rac1 GTPase binding domain of plexin-B1 has a ubiquitin fold. *J. Biomol. NMR* **31**, 369–370 (2005).
19. Y. Tong, P. Chugha, P. K. Hota, R. S. Alviani, M. Li, W. Tempel, L. Shen, H.-W. Park, M. Buck, Binding of Rac1, Rnd1, and RhoD to a novel Rho GTPase interaction motif destabilizes dimerization of the plexin-B1 effector domain. *J. Biol. Chem.* **282**, 37215–37224 (2007).
20. H. G. Vikis, W. Li, Z. He, K. L. Guan, The semaphorin receptor plexin-B1 specifically interacts with active Rac in a ligand-dependent manner. *Proc. Natl. Acad. Sci. U.S.A.* **97**, 12457–12462 (2000).
21. I. Oinuma, Y. Ishikawa, H. Katoh, M. Negishi, The semaphorin 4D receptor Plexin-B1 is a GTPase activating protein for R-Ras. *Science* **305**, 862–865 (2004).
22. I. Oinuma, H. Katoh, M. Negishi, Molecular dissection of the semaphorin 4D receptor plexin-B1-stimulated R-Ras GTPase-activating protein activity and neurite remodeling in hippocampal neurons. *J. Neurosci.* **24**, 11473–11480 (2004).
23. L. J. Turner, S. Nicholls, A. Hall, The activity of the plexin-A1 receptor is regulated by Rac. *J. Biol. Chem.* **279**, 33199–33205 (2004).
24. K. Uesugi, I. Oinuma, H. Katoh, M. Negishi, Different requirement for Rnd GTPases of R-Ras GAP activity of Plexin-C1 and Plexin-D1. *J. Biol. Chem.* **284**, 6743–6751 (2009).
25. P. Chardin, Function and regulation of Rnd proteins. *Nat. Rev. Mol. Cell Biol.* **7**, 54–62 (2006).
26. C. D. Nobes, I. Lauritzen, M. G. Mattei, S. Paris, A. Hall, P. Chardin, A new member of the Rho family, Rnd1, promotes disassembly of actin filament structures and loss of cell adhesion. *J. Cell Biol.* **141**, 187–197 (1998).
27. Y. Ishikawa, H. Katoh, M. Negishi, Small GTPase Rnd1 is involved in neuronal activity-dependent dendritic development in hippocampal neurons. *Neurosci. Lett.* **400**, 218–223 (2006).
28. Y. Ishikawa, H. Katoh, M. Negishi, A role of Rnd1 GTPase in dendritic spine formation in hippocampal neurons. *J. Neurosci.* **23**, 11065–11072 (2003).
29. G. Ahnert-Hilger, M. Höltje, G. Grosse, G. Pickert, C. Mucke, B. Nixdorf-Bergweiler, P. Boquet, F. Hofmann, I. Just, Differential effects of Rho GTPases on axonal and dendritic development in hippocampal neurones. *J. Neurochem.* **90**, 9–18 (2004).
30. A. Harada, H. Katoh, M. Negishi, Direct interaction of Rnd1 with FRS2β regulates Rnd1-induced down-regulation of RhoA activity and is involved in fibroblast growth factor-induced neurite outgrowth in PC12 cells. *J. Biol. Chem.* **280**, 18418–18424 (2005).
31. H. Katoh, A. Harada, K. Mori, M. Negishi, Socius is a novel Rnd GTPase- interacting protein involved in disassembly of actin stress fibers. *Mol. Cell. Biol.* **22**, 2952–2964 (2002).
32. Z. Li, C. D. Aizenman, H. T. Cline, Regulation of rho GTPases by crosstalk and neuronal activity in vivo. *Neuron* **33**, 741–750 (2002).
33. A. Y. Nakayama, M. B. Harms, L. Luo, Small GTPases Rac and Rho in the maintenance of dendritic spines and branches in hippocampal pyramidal neurons. *J. Neurosci.* **20**, 5329–5338 (2000).
34. W. C. Sin, K. Haas, E. S. Ruthazer, H. T. Cline, Dendrite growth increased by visual activity requires NMDA receptor and Rho GTPases. *Nature* **419**, 475–480 (2002).
35. K. Wennerberg, M.-A. Forget, S. M. Ellerbroek, W. T. Arthur, K. Burridge, J. Settleman, C. J. Der, S. H. Hansen, Rnd proteins function as RhoA antagonists by activating p190 RhoGAP. *Curr. Biol.* **13**, 1106–1115 (2003).
36. K. Wünnenberg-Stapleton, I. L. Blitz, C. Hashimoto, K. W. Cho, Involvement of the small GTPases XRhoA and XRnd1 in cell adhesion and head formation in early *Xenopus* development. *Development* **126**, 5339–5351 (1999).
37. P. K. Hota, M. Buck, Plexin structures are coming: Opportunities for multilevel investigations of semaphorin guidance receptors, their cell signaling mechanisms, and functions. *Cell. Mol. Life Sci.* **69**, 3765–3805 (2012).
38. S. M. Zanata, I. Hovatta, B. Rohm, A. W. Püschel, Antagonistic effects of Rnd1 and RhoD GTPases regulate receptor activity in semaphorin 3A-induced cytoskeletal collapse. *J. Neurosci.* **22**, 471–477 (2002).
39. I. Oinuma, H. Katoh, A. Harada, M. Negishi, Direct interaction of Rnd1 with Plexin-B1 regulates PDZ-RhoGEF-mediated Rho activation by Plexin-B1 and induces cell contraction in COS-7 cells. *J. Biol. Chem.* **278**, 25671–25677 (2003).
40. S. Ramaswamy, H. Markram, Anatomy and physiology of the thick-tufted layer5 pyramidal neuron. *Front. Cell. Neurosci.* **9**, 233 (2015).
41. S. Romand, Y. Wang, M. Toledo-Rodriguez, H. Markram, Morphological development of thick-tufted layer v pyramidal cells in the rat somatosensory cortex. *Front. Neuroanat.* **5**, 5 (2011).
42. O. O. Odunuga, V. M. Longshaw, G. L. Blatch, Hop: More than an Hsp70/Hsp90 adaptor protein. *Bioessays* **26**, 1058–1068 (2004).
43. L. E. R. de Souza, M. D. M. Costa, E. S. Bilek, M. H. Lopes, V. R. Martins, A. W. Püschel, A. F. Mercadante, L. S. Nakao, S. M. Zanata, STI1 antagonizes cytoskeleton collapse mediated by small GTPase Rnd1 and regulates neurite growth. *Exp. Cell Res.* **324**, 84–91 (2014).
44. Y.-H. Li, S. Ghavampur, P. Bondallaz, L. Will, G. Grenningloh, A. W. P. Schel, Rnd1 regulates axon extension by enhancing the microtubule destabilizing activity of SCG10. *J. Biol. Chem.* **284**, 363–371 (2009).
45. A. W. Püschel, GTPases in semaphorin signaling. *Adv. Exp. Med. Biol.* **600**, 12–23 (2007).
46. K. Matsumoto, T. Asano, T. Endo, Novel small GTPase M-Ras participates in reorganization of actin cytoskeleton. *Oncogene* **15**, 2409–2417 (1997).
47. A. C. Kimmelman, N. N. Rodriguez, A. M.-L. Chan, R-Ras3/M-Ras induces neuronal differentiation of PC12 cells through cell-type-specific activation of the mitogen-activated protein kinase cascade. *Mol. Cell. Biol.* **22**, 5946–5961 (2002).
48. N. N. Rodriguez, I. N. L. Lee, A. Banno, H. F. Qiao, R. F. Qiao, Z. Yao, T. Hoang, A. C. Kimmelman, A. M.-L. Chan, Characterization of R-ras3/m-ras null mice reveals a potential role in trophic factor signaling. *Mol. Cell. Biol.* **26**, 7145–7154 (2006).
49. Y. Saito, I. Oinuma, S. Fujimoto, M. Negishi, Plexin-B1 is a GTPase activating protein for M-Ras, remodelling dendrite morphology. *EMBO Rep.* **10**, 614–621 (2009).
50. G.-I. Tasaka, M. Negishi, I. Oinuma, Semaphorin 4D/Plexin-B1- mediated M-Ras GAP activity regulates actin-based dendrite remodeling through Lamellipodin. *J. Neurosci.* **32**, 8293–8305 (2012).
51. P. Sun, H. Watanabe, K. Takano, T. Yokoyama, J.-i. Fujisawa, T. Endo, Sustained activation of M-Ras induced by nerve growth factor is essential for neuronal differentiation of PC12 cells. *Genes Cells* **11**, 1097–1113 (2006).
52. B. Q. Zhuang, Y. R. S. Su, S. Sockanathan, FARP1 promotes the dendritic growth of spinal motor neuron subtypes through transmembrane Semaphorin6A and PlexinA4 signaling. *Neuron* **61**, 359–372 (2009).
53. K. Riento, R. M. Guasch, R. Garg, B. Jin, A. J. Ridley, RhoE binds to ROCK I and inhibits downstream signaling. *Mol. Cell. Biol.* **23**, 4219–4229 (2003).
54. J. Aoki, H. Katoh, K. Mori, M. Negishi, Rnd1, a novel rho family GTPase, induces the formation of neuritic processes in PC12 cells. *Biochem. Biophys. Res. Commun.* **278**, 604–608 (2000).
55. R. J. Pasterkamp, R-Ras fills another GAP in semaphorin signalling. *Trends Cell Biol.* **15**, 61–64 (2005).
56. Y.-Y. Wang, N. Han, D.-J. Hong, J. Zhang, Nogo-A aggravates oxidative damage in oligodendrocytes. *Neural Regen. Res.* **16**, 179–185 (2021).
57. A. B. Huber, A. Kania, T. S. Tran, C. Gu, N. D. M. Garcia, I. Lieberam, D. Johnson, T. M. Jessell, D. D. Ginty, A. L. Kolodkin, Distinct roles for secreted semaphorin signaling in spinal motor axon guidance. *Neuron* **48**, 949–964 (2005).
58. M. M. Bradford, A rapid and sensitive method for the quantitation of microgram quantities of protein utilizing the principle of protein-dye binding. *Anal. Biochem.* **72**, 248–254 (1976).
59. J. Zhang, K. Wei, W. Qu, M. Wang, Q. Zhu, X. Dong, X. Huang, W. Yi, S. Xu, X. Li, *Ogt* deficiency induces abnormal cerebellar function and behavioral deficits of adult mice through modulating RhoA/ROCK signaling. *J. Neurosci.* **43**, 4559–4579 (2023).
60. D. A. Sholl, Dendritic organization in the neurons of the visual and motor cortices of the cat. *J. Anat.* **87**, 387–406 (1953).
61. E. Meijering, M. Jacob, J.-C. F. Sarria, P. Steiner, H. Hirling, M. Unser, Design and validation of a tool for neurite tracing and analysis in fluorescence microscopy images. *Cytometry A* **58**, 167–176 (2004).
62. B. Lom, S. Cohen-Cory, Brain-derived neurotrophic factor differentially regulates retinal ganglion cell dendritic and axonal arborization in vivo. *J. Neurosci.* **19**, 9928–9938 (1999).

Acknowledgments: We thank J. P. Zanin and W. Friedman (Rutgers University) for providing the plasmids. We thank J. P. Zanin, V. Danelon, and E. Martinez (Rutgers University) for expert technical assistance. **Funding:** This work is supported by the NJ Governor's Council for Medical Research and Treatment of Autism (CAUT17BSP022) to T.S.T. and NSF/IOS (1556968 and 2034864) to T.S.T. and A.Y., who is also supported as an incumbent of the Jack & Simon Djanogly Professorial Chair in Biochemistry. **Author contributions:** T.S.T. and A.Y. conceptualized and designed the research. O.A. performed most of the experiments. T.S.T., A.Y., and O.A. analyzed the data and interpreted the results. J.B. conducted additional experiments and assisted with preparing the figures. O.A. prepared most of the figures and wrote the first draft of the manuscript. T.S.T. and A.Y. edited the final manuscript and figures. **Competing interests:** The authors declare that they have no competing interests. **Data and materials availability:** All data needed to evaluate the conclusions in the paper are present in the paper or the Supplementary Materials.

Submitted 13 March 2023
Accepted 21 December 2023
Published 16 January 2024
10.1126/scisignal.adh7673